

The Rhône River Prodelta: Short-Term (10^0 – 10^3 Year) Sedimentation Patterns and Human Impact

Abdelali Touzani and Pierre Giresse

Laboratoire de Sédimentologie Marine
University of Perpignan
Avenue de Villeneuve
66860 Perpignan, France

ABSTRACT

TOUZANI, A. and GIRESSE, P., 2002. The Rhône River prodelta: short-term (10^0 – 10^3 year) sedimentation patterns and human impact. *Journal of Coastal Research*, 18(1), 102–117. West Palm Beach (Florida), ISSN 0749-0208.



We compared various data sets obtained on the Rhône River delta and the adjacent land over the past 1000 years. Data sources were historical documentation and quantitative results. The period of the Rhône d'Ulmet (before 1300 y. A.D.) corresponds to the north-western position of the river mouth and to climatic and runoff variations of low magnitude. In the prodelta area, mottled muds are common and laminated muds were not observed due to the distance of collected data from the mouth. The "wild" Rhône period from 1587 to 1869 y. A.D. (Bras de Fer and Grand Rhône mouths) shows a dramatic extent (7–8 km distance) of laminated muds resulting from seasonal floods. Changes in climatic conditions probably modified the watershed and played a prominent part in the prodelta development. During this period, pedogenic ochre aggregates were reworked from swamp soils of the delta during channel migrations. In all our cores, the top of laminated muds coincides with the disappearance of the ochre aggregates. The Recent period of the Rhône channeling began with the 1869 rectification which fixed the main channel. The consequence was a drastic reduction of laminated muds to a 3–4 km proximal area off the stabilized mouth. With a decrease in flood supply and a longer time of exposure, we can observe a coarsening trend in the upper part of the cores as a result of repetitive reworking processes. The seasonal build-up of laminites is altered seaward: faintly laminated muds and mottled muds deposition shifted with increasing distance from the river mouth. Markers of the anthropogenic pollution, such as metallurgic microballs (Fe sulfides) and talc characterized the upper third of the cores.

A variety of previous sedimentological data and ^{210}Pb and ^{137}Cs age estimates indicate very fast sediment accumulation rates in the proximal Rhône prodelta (30 – 40 cm y^{-1}) which would be regarded as apparent rates. Detailed investigation of the gravity cores located off the Rhône River mouth showed marked coarsening-upward trends (condensed section), clast deposition, and truncated structures that indicate the processes of sea floor erosion and reworking. On the distal Rhône prodelta, a thin recent veneer overlies the Holocene tract of the initial transgression and indicates a hiatus of ≈ 5 – 6000 y. Decreased discharge and reworking have been especially obvious since 1950, resulting from both the developing hydroelectric catchment and the decrease in winter rainfall.

ADDITIONAL INDEX WORDS: Rhône River, prodelta, human impact, laminite, ^{210}Pb , deforestation, microtidal.

INTRODUCTION

The Rhône River drainage basin is one of the largest catchments in Europe, whose importance was recognized by ancient civilizations. Today it is a heavily populated industrialized basin. The flow of this river and especially its solid input to the sea has changed as a result of river works (flood protection, irrigation and agricultural land drainage). The history of its delta interlaces with the history of Man seeking to protect himself from flood or to enhance navigation. The most obvious change was the hydroelectric development undertaken since 1950. But changes in natural parameters controlling the water supply were also recorded since the beginning of the observation period, namely the 19th century (VIVIAN, 1989; PROBST, 1989). They are grouped into two categories: the first one including all changes in the runoff patterns resulting from glacial dynamics, since the snowline of the Alps has decreased by about 25 % from the beginning of the

19th century. The second one is the change of the rainfall regime since the beginning of this century (especially winter rainfall, which decreased since 1950 compared to long-term average).

Older historical changes also have natural and anthropogenic causes. The latter were never as effective as during the last century, but deforestation and cultivation spread between 500 and 1300 y. A.D., according to maps and archives (BRAVARD and BÉTHEMONT, 1989). Various authors recognized the potential role of various processes: fluvial transport, shore erosion, plume dispersion and Late Quaternary evolution of the deltaic fringe have been the focus of much interest (e.g. ALOISI *et al.*, 1994; BLANC et JEUDY DE GRISSAC, 1982; DEMARCQ and WALD, 1984; ESTOURNEL *et al.*, 1997; PROVANSAL and MORHANGE, 1994). However the respective contribution of these processes to the small-scale evolution of the Rhône River prodelta is poorly known. Because the nature of this short-term accumulation cannot be understood without a prior ^{210}Pb chronology, the most recent (1000 yr) history remains poorly understood.

For this sedimentological work, we analyzed in detail var-

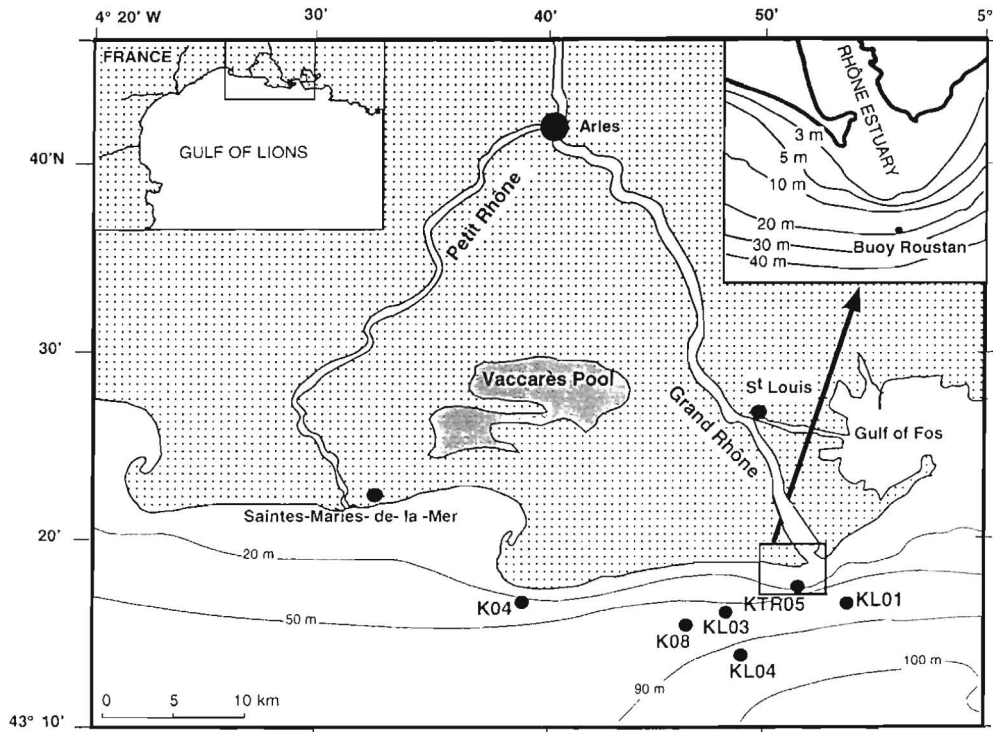


Figure 1. Bathymetric map of the study area showing the location of coring stations.

ious cores sampled in the subaqueous prodelta area of the Rhône River (Figure 1). We focused on the laminated microstructures of the proximal area, and particular attention was paid to the relationship between sediment accumulation rate and frequency of seasonal flooding. We also studied the seaward spreading of the suspended load and the migration of the main deltaic lobes during the last centuries. Sedimentary structures form as a result of the complex interaction between particle supply, as well as oceanic physical and biological processes active in a locale at present and/or after the time of deposition. The purpose of this paper is (1) to evaluate the spatial distribution of the present sedimentary supply of the river within the proximal and distal areas of the mouth, and (2) to determine the historical changes of sediment accumulation during the last millennium, and especially the relative influence of natural and anthropological factors.

PHYSICAL SETTING

The Rhône River is 812 km long (WELCOMME, 1978) and with the average water discharge is about $1700 \text{ m}^3 \text{ s}^{-1}$, ranks 42th in the world. Its total drainage area is about 97800 km^2 , one of Europe's largest catchments. Its hydrological regime is markedly influenced by the Alps and Jura Mountains. The Rhône River prodelta is the submarine part of the delta and is extended through the inner part of the shelf. Its accumulation was studied in the upper part of the High Sea-Level Tract which is still evolving today (GENSOUS and TESSON, 1996).

Discharge Characteristics and Sediment Load

The water discharge of the Rhône River ranges from $1063 \text{ m}^3 \text{ s}^{-1}$ to $2376 \text{ m}^3 \text{ s}^{-1}$ (with one tenth from the Petit-Rhône mouth) (Figure 1). Typically, water discharge is maximum in November and January–February and minimum in the summer (PONT, 1993; 1997). Maximum discharge is four times greater than minimum, because various segments situated in different geographic and climatic settings, flood at different periods of the year. Consequently, this river exhibits large temporal fluctuation. The Rhône River carries an estimated average amount of $5 \times 10^6 \text{ t y}^{-1}$ to $8.5 \times 10^6 \text{ t y}^{-1}$ estimated by SAVEY and DELÉGLISE (1967) and RODITIS and PONT (1993) respectively. Recent estimations of the solid discharge between 1980 and 1991 indicated that the annual discharge varies between 2.6 and $19 \times 10^6 \text{ t y}^{-1}$ (PONT, 1997). During 1994–95, $14 \times 10^6 \text{ t}$ of suspended matter reached the sea (whose $11 \times 10^6 \text{ t}$ corresponding to the flood discharge) (WALTER *et al.*, 1997). Part of the sediment load is sand transported along the river bed. It can roughly be estimated as 0.1 to $0.2 \times 10^6 \text{ t y}^{-1}$ (SOGREAH, 1994). The Rhône River is the major source of particulate matter which constitutes more than 80% of the total fluvial supply to the Gulf of Lions (ALOISI *et al.*, 1979).

Oceanographic Processes

The delta is characterized by microtidal conditions with a maximum tidal range of 0.4–0.5 m and the most common

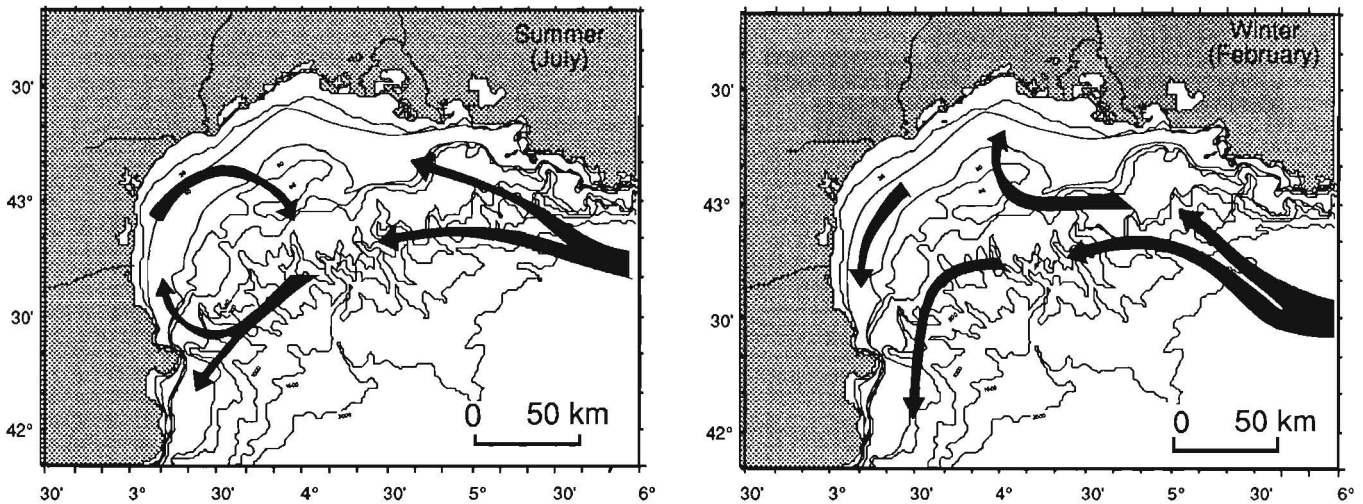


Figure 2. Schematic representation of the regional water circulation in summer (July) and winter (February) after THUNUS (1996).

wave height 1–1.5 m. The waves greater than 4 m are uncommon (BLANC and JEUDY DE GRISSAC, 1982). In this part of the Gulf of Lions, the general circulation is represented by the Liguro-Provençal-Catalan Current, (LPC or Northern Current). This current flows alongside the Côte d'Azur and the Gulf of Lions following the shelf break and reaches the Catalanian coast (Figure 2; THUNUS, 1996). The velocity of associated currents is a few cm s^{-1} (MILLOT, 1990). However, sedimentation patterns are clearly controlled by this circulation, which transports the Rhône material to the southwest. Two types of winds are predominant in the area: the north-west sector winds (mistral) blow all year around and induce upwelling especially along the coast of the Rhône delta. The prevailing east sector winds are more frequent in autumn and spring and may induce downwelling. DEMARCQ and WALD (1984) have not observed the influence of the LPC current on the deviation of the plume, which they related primarily to the wind forcing. ESTOURNEL *et al.* (1997) established that the overall orientation of the plume is subjected to winds and surrounding circulation, with coastal currents associated with upwelling and downwelling. The suspended matter of the plume can rapidly settle in the prodelta zone: it is assumed that 75% of the mass is deposited within a 3-mile limit off the river mouth (ALOISI *et al.*, 1979). The annual prodeltaic accumulation of $2 \times 10^6 \text{ t y}^{-1}$ represents a quarter of the mass accumulated in the mid shelf mud belt ($8 \times 10^6 \text{ t y}^{-1}$, DURRIEU DE MADRON *et al.*, 2000). DURRIEU DE MADRON and PANOUSE (1996) showed that the bottom nepheloid layer on the shelf persists throughout the year.

Morphology of the Prodelt

The sub aqueous delta extends from the shoreline to a 80–90 m depth of with a flat gently sloping sea floor (0.004–0.005). The only elevated morphology *e.g.* features are the sandy bars and the channels in front of the river mouth. It seems difficult to divide this prodelta into an upper and a lower part according to the bathymetry: the only figure of

accretion is indicated by a modest convexity of the 20 m isobath (Figure 1). As for the Tiber delta area (ALESSANDRO *et al.*, 1990), the prodelta slope can be divided on the basis of the sedimentation rates. The upper prodelta slope (topset beds) is characterized by high rate of sedimentation ($>30 \text{ cm y}^{-1}$) and the lower prodelta slope (topset and foreset beds) is characterized by a lower rate ($<30 \text{ cm y}^{-1}$). The absence of morphological break suggests that over a large part of the upper slope, condensed sections are the result of alternating phases of suspension and erosion, associated with intensified surface waves superimposed on ambient currents.

PREVIOUS WORK

Historical Evolution of the Rhône River and Delta

The literature on the Rhône River valley is mainly geological, which provides useful information on environmental evolution over the past 2500 years. During this period, progressive human interferences with physical processes include either soil erosion and water retention in the hydrological basin or drains, embankments and dams.

Climatic data of the Northern Hemisphere show a succession of warm and cold phases over the last 3000 years which resulted in dry and wet periods in the Mediterranean area. A climatic system with intensive abundant precipitation characterizes the first part of the first millennium B.C. and the 15–19 A.D. Little Ice Age, while the Roman time (300 B.C.—500–600 A.D.) appears as a relatively dry period. The Late Holocene morphogenic evolution is particularly well documented in the Basse Provence area (PROVANSAL and MORHANGE, 1994).

(1) A wet period encompasses the beginning of the Bronze Age and during the Iron Age (between the 6th and the 3rd century B.C.). During this period, the evolution included a synchronic embankment of thalweg and accumulation in littoral plains, then the progradation of the deltaic shoreline.

(2) During the Roman Age (300 years B.C. to 500–600 years

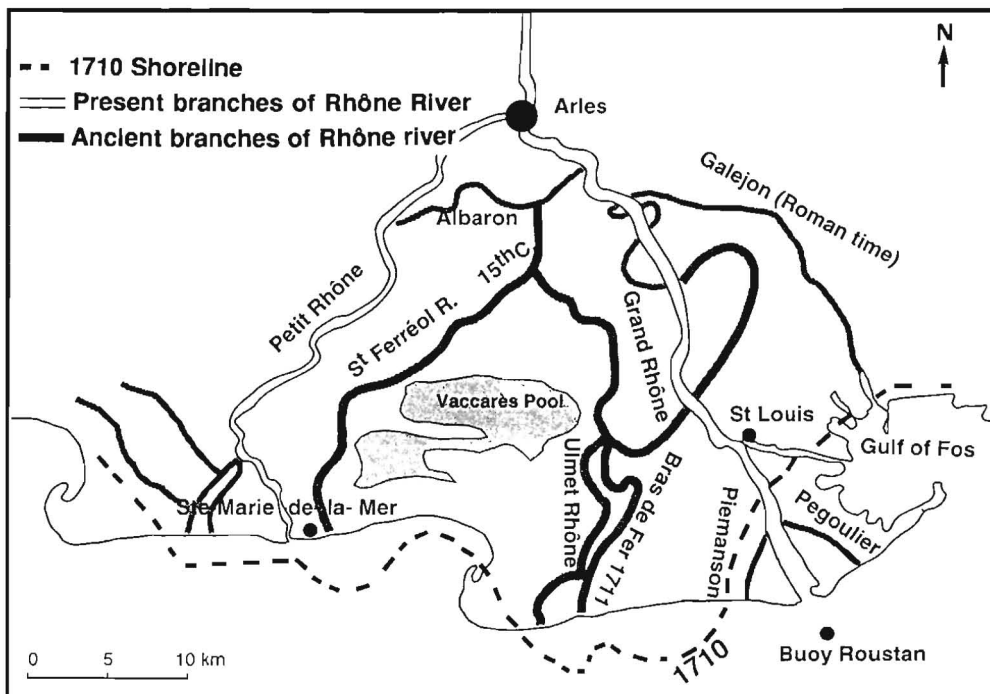


Figure 3. General configuration of former major Rhône River distributaries (after DUBOUL-RAZAVET and KRUIT, 1957 and L'HOMER *et al.*, 1981).

A.D.), erosion was moderate. This observation may be related to a climatic pause, as opposed to an increasing human occupation.

(3) The following phase of the medieval period, ending in the 15th century, was relatively warm with various torrential flows, a decrease of agriculture, and forest exploitation is growth. The same intermediate phase was also described in the Tiber basin (BELLOTI *et al.*, 1994).

(4) The relatively cold phase between the 15th and 19th centuries corresponded to a short cooling phase named "the Little Ice Age" (LAMB, 1966). Floods were much more frequent and intense and the progradation rate of the deltaic shoreline increased. However, this trend was also reinforced by human activities, either in the drainage or in the deltaic areas. Sediment supply increased remarkably as the result of deforestation and agriculture as in other large deltaic areas: the Nile River (COUTELLIER and STANLEY, 1987) and the Yellow River (MILLIMAN *et al.*, 1987). During the past century, human activities have increased remarkably and produced a relative decrease in sediment supply through reforestation, dam-building and river-bed quarrying as in other Western Mediterranean rivers (Tiber River; ALESSANDRO *et al.*, 1990, Ebro River; VARELA *et al.*, 1986).

Consequently, progradation and lobe migration processes are genetically related since they are linked to sediment supply during the successive climatic phases. Previous papers proposed a tentative chronology of the high-frequency climatic-morphogenetic oscillations which control the progression of successive subdelta lobes (DUBOUL-RAZAVET and KRUIT, 1957; BLANC, 1977; L'HOMER *et al.*, 1981; 1992). From the

Neolithic to the Middle Age, at least three branches crossed the lower delta plain (Ulmet Rhône, Albaron, and Saint-Ferreol branches) (Figure 3). Precise mapping of some ancient branches is difficult because channels shifted laterally (an eastern branch, the Galejon branch, was described during the Roman time). Then Ulmet Rhône was abandoned during the 13th century because at both new channel system building and climatic shifting (wet episode before the Little Ice Age, BRAVARD, 1983). Finally, the number of the main distributaries reduced to two major branches, the Saint-Ferreol Rhône (15th century mostly) and the Bras de Fer which became the main channel (1587–1711). During the great flood of 1711, a lateral shifting to the east occurred: the present Grand Rhône was established while flow diminished in the earlier channel system (Petit-Rhône). Throughout the 19th century, the mouth of the Grand Rhône was unstable with two active branches (Pegoulie and Piemanson) (Figure 3). In 1869, the channel of the Grand Rhône was dug and the main mouth was nearly stabilized in its present position (VIVIAN, 1989). The latest subdelta lobes can be recognized along the present shoreline, from west to east: Saint-Ferreol, Bras de Fer, Piemanson and Pegoulie. The present lobes off Grand Rhône and Petit-Rhône are quite small because the input of sandy material decreased due to the recent structural developments (dams, dykes, etc).

²¹⁰Pb Chronology and Accumulation Rates

Sediment accumulation rates of various prodeltaic cores of the area, especially those of the present study, were deter-

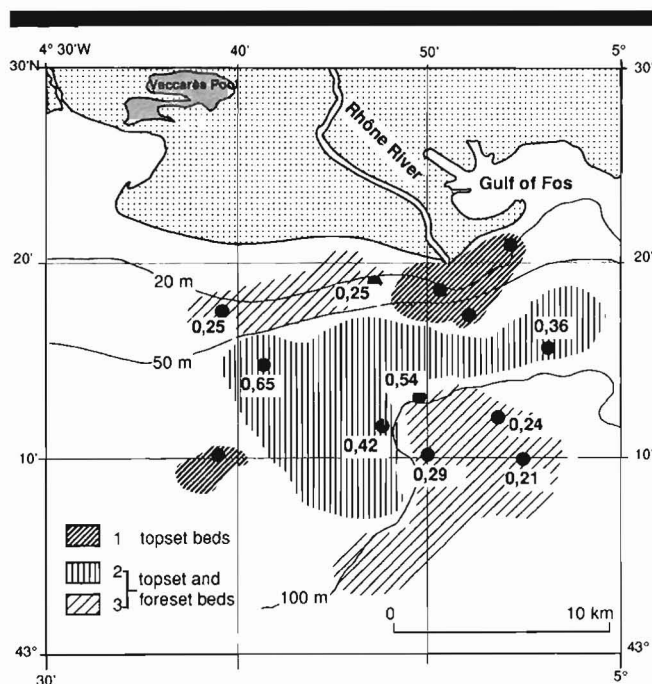


Figure 4. Areal distribution of mean sediment accumulation rates according to ^{210}Pb profiles (after measurements of RADAKOVITCH *et al.*, 1998), 1—irregular occurrence of ^{210}Pb activity, 2—downcore exponential decrease activity, 3—irregular occurrence of ^{210}Pb activity in the topbeds, then downcore decreasing activity.

mined using both ^{210}Pb and ^{137}Cs geochronological methods (RADAKOVITCH, 1995; RADAKOVITCH *et al.*, 1999). In the shallower part of the prodelta area ($<40\ \mu\text{m}$), ^{210}Pb activity revealed a sedimentation rate too high to be measured ($>30\ \text{cm y}^{-1}$). This is a consequence of bottom sediment resuspension by wave action and successive fluvial input. In the distal part of the prodelta, vertical activity gradients were used to estimate a sedimentation rate ranging from 0.36 to 0.65 cm y^{-1} . Less regular profiles were observed at both the west part of the mouth and the upper slope where the area of deposition is controlled by biological mixing. Lower sedimentation rates (0.21–0.29 cm y^{-1}) were restricted to the upper slope (Figure 4).

METHODS

The data set consists of 6 gravity cores with an average spacing of 5 km and depths in the range of 4 and 7 m. Cores were split lengthwise and sampled at intervals of 5 cm or less in order to sample between all lithological boundaries. Sub-samples of the sediment structures were collected in 5×3 cm plastic boxes and impregnated with low-viscosity resin for thin section analysis.

The sand was separated by wet-sieving at $50\ \mu\text{m}$, and silt and clay fractions were analyzed with a Sedigraph 5100 (Micromeritics). A binocular microscope was used to establish the types of particle assemblages and to observe various environmental markers of marine sedimentation (benthic foraminifers, echinoid debris, glauconitic grains) and of terrige-

nous supply (vegetal fragments, aggregates reworked from the deltaic plain, beach sandstone debris or metallurgic microballs). The proportions of the most characteristic markers were estimated. Grain-size analyses were performed using standard sieving techniques. A Scanning Electronic Microscope (SEM) Hitachi coupled with an E.D.V.R. Tracor was used for studying the shape and composition of selected particles. Mineralogical analysis was performed by X-ray diffraction on the fraction finer than $2\ \mu\text{m}$, on selected particles. Organic and inorganic carbon contents were analyzed using a Leco induction furnace (total carbonate = inorg. carbon \times 8.33).

Sediments accumulation rates were calculated using ^{210}Pb at the same sample sites as RADAKOVITCH (1999). Pollen assemblages were examined in three cores and will be discussed elsewhere (SUC *et al.*, in preparation).

RESULTS

Spatial Distribution of Lithofacies and Sedimentary Structures of Surficial Sediments

Proximal muds grade into distal muds approximately 10 km from River mouth. This change is characterized by a grain-size decrease toward the outer part of the shelf. The sandy fraction reaches about 30% 3 km off the mouth, decreases to 15% at 8 km, and is minimal (0–5%) from 10 km to the shelf break (Figure 5a). Conversely, we observe a gradual increase in carbonate content toward the outer part of the prodelta (Figure 5b). The carbonate content varies from a minimum of 30% less than 5 km off the mouth to a maximum of 38% 15 km from the mouth. The major part of carbonates is of detrital origin from the modern alluvial flats (SCHMITTNER and GIRESE, 1999), and the minor part is of biogenic origin. The suspended matter of the Rhône River were collected to a distance of 20 km off the mouth and revealed that carbonate content is about 40% (PONT, 1992). These detrital carbonates are micritic aggregates ranging from 1 to $10\ \mu\text{m}$ in size. The conditions of deposition are optimal in the finest distal muds. However, the carbonate content decreases seaward of 15 km from the mouth, as a result of an increased sorting and accumulation of the finest aluminosilicate particles. This distribution indicates that the influence of oceanic biogenic carbonates is minor at this scale. The profile of organic carbon is similar to that of sand fraction (Figure 5c). Unlike the usual grain size concentration of organic particles in the fine fraction, the organic carbon content is higher in the coarser proximal muds than in the distal muds. This difference is due to the abundance in the proximal muds of dark vegetal debris whose grain size ranges from 40 to $100\ \mu\text{m}$. On the basis of these analyses, three main lithofacies were distinguished from the shallow area toward the outer shelf.

Proximal Laminated Mud

Today, these deposits are restricted to a half-circle extending 4–5 km seaward off the mouth (Figure 6a). Sediment accumulated as well-laminated with repetitive couplets of plane light grey microlayer and dark grey microlayer, tenths of mil-

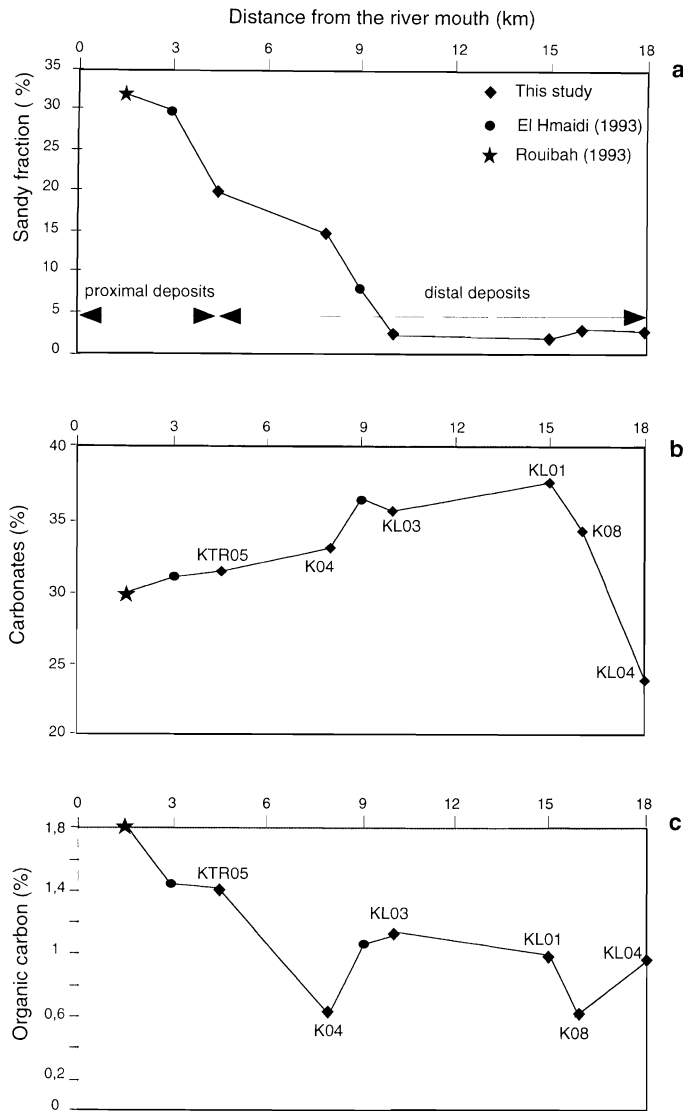


Figure 5. Seaward variations of sandy fraction (a), carbonates (b) and organic carbon (c) contents in the surficial deposits of the Rhône prodelta. The proposed boundary between proximal and distal facies is based on sand %.

limeters to several centimeters thick. Dark-colored microlayers are coarser (the sand fraction represents 30 to 40%) and more organic (> 1.5% organic carbon) (Figure 7d). The light color is due to two types of material: organic matter, that decreases (Figure 7d), and micritic carbonate concentration which increases (up to 30 %)(Figure 7a). The cumulative curve pattern of the dark laminae is usually a regular, bended form with an upward concavity (parabolic curve of RIVIÈRE, 1977 and BALTZER, 1980). It is interpreted as representing a short transportation from the source and a weakening of the fluid competency in a less energetic setting. The light laminae cumulative curves are convex with a downward concavity (hyperbolic curve of the same authors) and appear to be the result of a slow settling from a quiet water column. Transition from dark lower laminae to light upper laminae

can be either sharp or gradational. While in some cases, sharp erosional contact are observed at the top of the light upper laminae. The laminae are laterally continuous, parallel to sub-parallel. In some cases, the thicker dark laminations pinch out laterally and show low-angle cross-bedding (Figure 8a). Bioturbation and degradation of physical structures is slight or absent. Some soft sediment deformation structures are observed in the light laminae when they are overlain by sandy muds. These load features usually indicate that sediment deposition rates were high (BRENCHLEY and NEWALL, 1977; JAEGER and NITTROUER, 1994). Intervals without any sedimentary structures were found to be several centimeters in thickness. Some intervals reveal an atypical composition with coarser light laminae and clay-rich dark laminae.

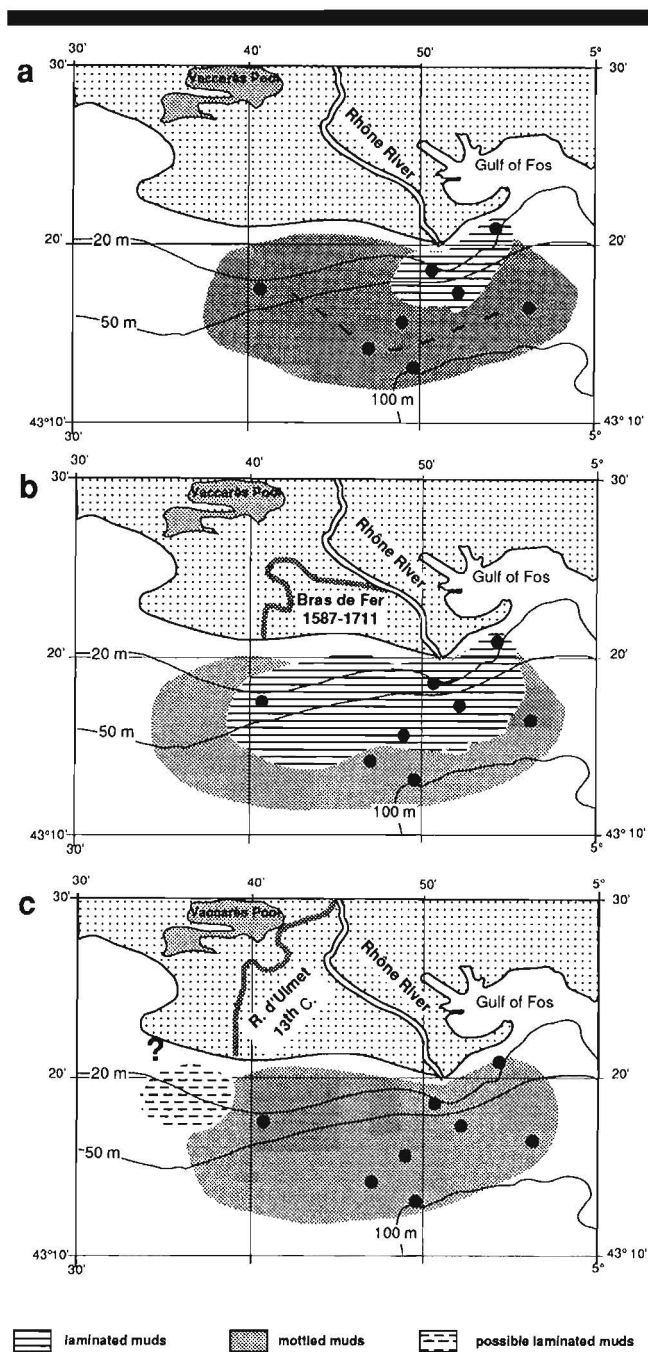


Figure 6. Evolutionary trend of laminite sedimentary structure deposition in the Rhône prodelta., a.) present pattern (a broken line indicates the boundary between the inner faintly laminated muds and the outer mottled muds), b.) Bras de Fer period (1587–1711 y. A.D.), c.) Rhône d'Ulmet period (before 1300 y. A.D.)

Faintly Laminated Mud

These deposits are accumulating as shallow area from 5 to 9 km off the mouth; this type of deposit is not represented on the map but its outer boundary is schematically indicated on Figure 6a. Rhythmic deposits are restricted to wide dark

layers whose thickness is inframillimetric. The grain size definition of these layers cannot be determined. The dark organic pigment is useful to match profiles. In general, light layers cannot be distinguished in the fine mud matrix. The undulating laminates are spaced with 2–30 cm intervals and might represent lag layers remaining after erosional events. These deposits are characterized by wavy laminae, sharply truncated either at the top or at the base of the layers, and mud chip intraclasts (Figure 8b c, d). These usually organic intraclasts are generally oriented parallel to the layering and poorly sorted. Although primary sedimentary structures dominate this facies, there were some evidence of bioturbation by generally mud feeding echinoids. Regularly, the degree of bioturbation increased seaward from the river mouth. Similar trends were reported for the Amazon sub aqueous delta (KUEHL *et al.*, 1995).

Mottled Mud

Mottled muds accumulate in the outer part of the prodelta (Figure 6a). They are grey homogeneous mud with dark-colored spots. They are characterized by mottling and lower proportions of vegetal-rich layers compared to proximal muds (although small plant fragments are abundant and ubiquitous). The dark-colored spots were scattered throughout the deposit, and were not related to grain-size fluctuations. Mottled muds occasionally contain bioturbation reworking structures by subsurface deposit feeders. Debris of mud feeding echinoids (spines, sterom-fragments) are fairly common.

Short-Term Sedimentation (Yearly Time Scale)

Deposits in the proximal area of the Rhône prodelta are characterized by laminated mud. The contrasts in color and in lithology in Core KTR05 was used to record the detailed seasonal distribution of pollen (SUC *et al.*, in preparation).

40–17 cm Interval (Figure 9a)

The lower (5 cm) this interval includes abundant Cupressaceae and riverain vegetation pollens, suggesting a deposition phase during a winter-spring period. The increase of grass plants over about 15 cm, indicates that the layer was contemporaneous with a summer-autumn period. Lastly, the distinct decrease of grass plants, above 20 cm, indicates the beginning of a new cold season. The vertical profile of sand fraction indicates that sediment deposited in winter was coarser (summer sand content was multiplied by two). According to the palynological record, autumn floods were likely to have produced this detrital accumulation. The light gray summer layers showed higher carbonate content (>27%) than the dark gray winter layers (<27%) (Figure 7a,b). Generally, organic carbon contents decreased with increasing carbonate content. This effect may be due to both siliclastic and organic composition of the flood sediments.

117–90 cm Interval (Figure 9b)

The variation of the pollen assemblage was found consistent with a nearly entire seasonal cycle record. The boundary between spring and summer periods was indicated by the in-

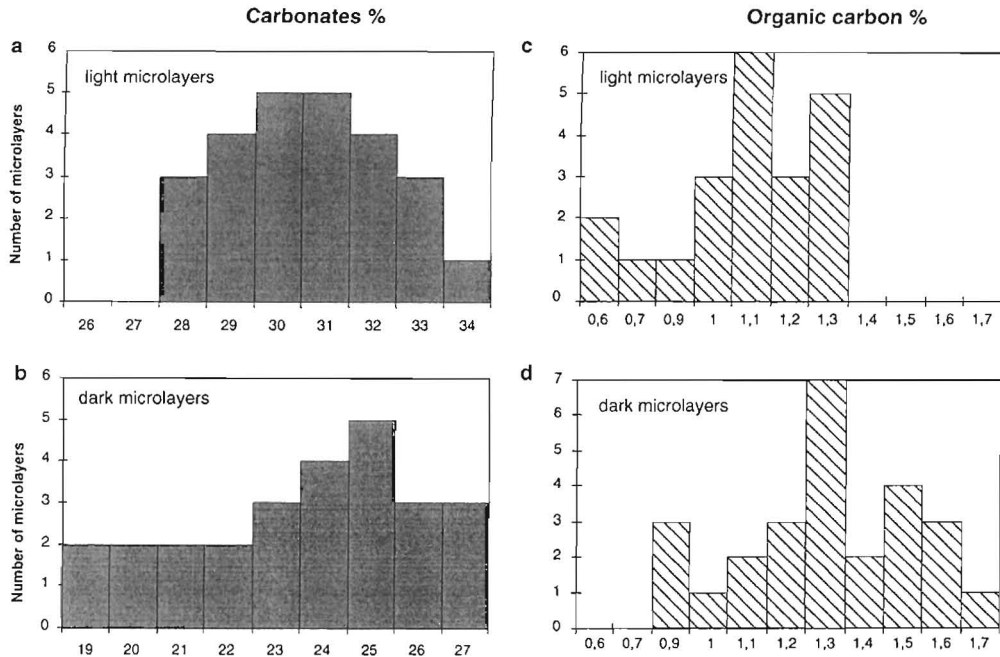


Figure 7. Comparative distribution of carbonate (a) and organic carbon (b) contents in dark and light layers of laminite sequences;

creases of both grass plants and halophyte pollens. In contrast, riverain vegetation pollens predominantly occurred during the high winter flows. Between 108 and 94 cm, two peaks of grass plant and halophyte were recorded in the summer interval. The last winter period was suggested, marked by higher Cupressaceae pollens with associated riverain vegetation representatives. Dark layers correspond to the spring (107–108.5 cm) and summer (102–100.5 cm, 95–94 cm) periods. Only the 102–100.5 cm layer shows a sand fraction associated with organic carbon. This event is assumed to correspond to a flood of late spring given the pollen assemblage of riverain vegetation origin associated with summer indicators. However, the pollens association of the 108–107 cm dark layer is not consistent with a major winter flood and should rather be interpreted as reworking. Small silty lenses within light mud layers are clear evidence for reworking processes. Thus the carbonate concentration on the summer layers is not observed in this interval.

The vertical distribution of the laminated facies is a record of seasonal sediment accumulation. Physical processes (reworking, winnowing) affected the proximal area at least occasionally (condensed sections or mixed layers). However, the higher organic carbon content in the dark layers of flood and the higher carbonate content in the light summer layers indicate that the effect of flood sedimentation was not entirely overprinted.

Modern Sedimentation (Annual Time Scale)

Description. Core KL03 was recovered by about 10 km from the mouth of the Rhône River at 79 m water depth, in an area where the average accumulation rates were estimated

at 0.5 cm y^{-1} according to ^{210}Pb datings (RADAKOVITCH *et al.*, 1999). It was selected as a type core because it presents the complete lithofacies succession of prodelta from base to top: (1) a lower mottled mud (LMM) with dark spots (440 to 350 cm), (2) a laminated mud (350–80 cm) (LM), and (3) an upper mottled mud (UMM) with dark spots (80 cm to the top) (Figure 10).

The sandy fraction content is generally lower than 2%, but increases slightly above 140 cm, near and above the top of the LMM. The organic carbon content shows a nearly similar vertical trend with values lower than 1% below 140 cm and higher than 1% above 140 cm. The vertical profile of carbonate content is uniform, with a slight increasing upward trend from 30 to 35%.

Under the binocular microscope, the sandy fraction displays several environmental markers:

—several benthic foraminifers, especially Milioliidae, Rotaliidae, Elphidiidae and debris of mud-feeding echinoids are abundant in the LMM, then become scarce in the lower part of LM. This marked decrease would be linked to a change in environmental conditions (increase in the accumulation rate?).

—green glauconitic grains are closely associated with benthic shells. This distribution can best be attributed to long residence time at the water-sediment interface linked to slow accumulation rate.

—ochre clayey aggregates were displaced from hydromorphic soils (or gleysols) of marshy area of the delta. Most notable among the hydromorph processes are the partial reduction of iron and manganese and the deposition of elemental sulphur, called thion (Figure 11a,b). This results in a “thionic

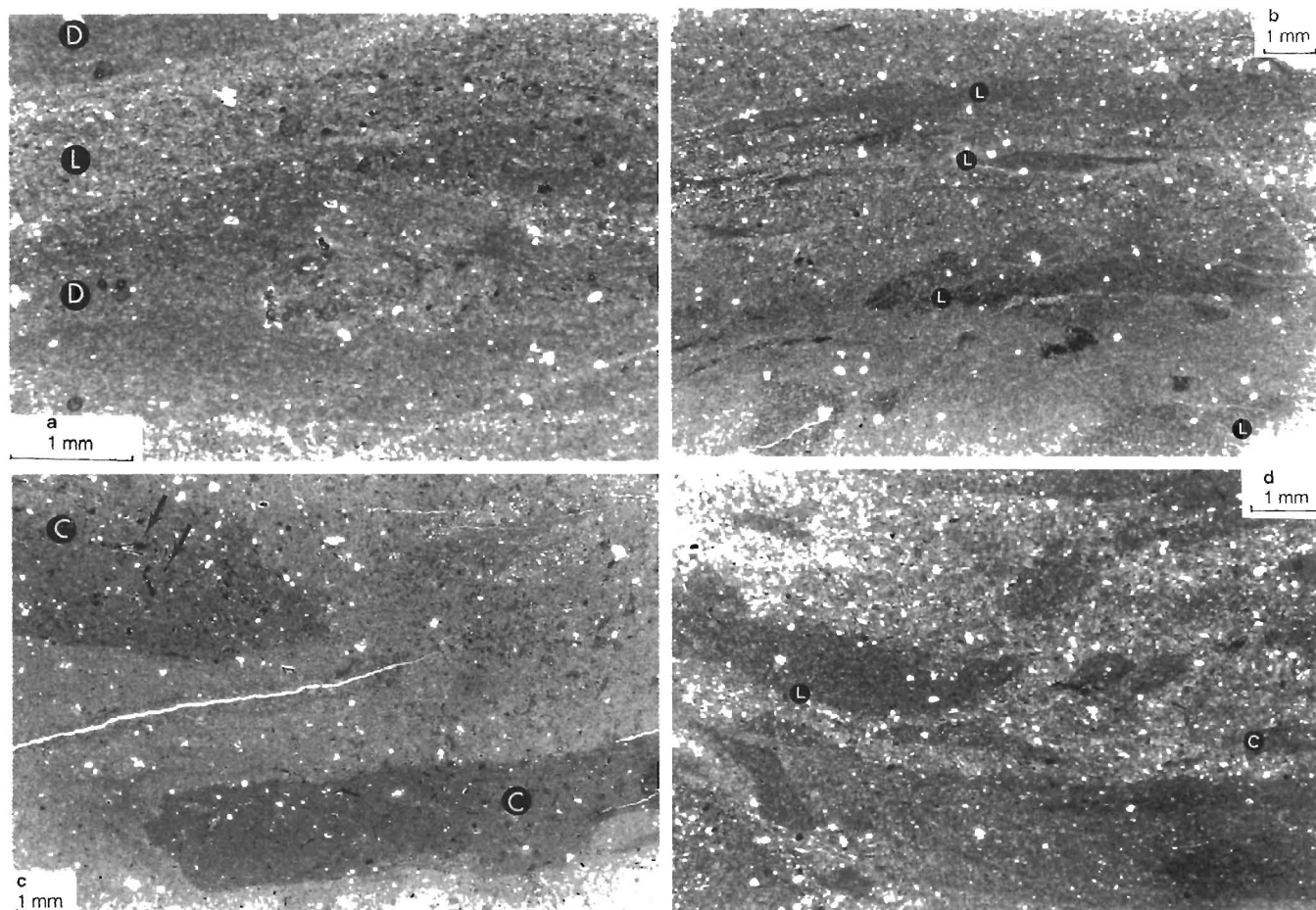


Figure 8. Photomicrographs of selected thin sections showing the microstructures described in the text. a: set of laminae composed of dark (D) organic siltstone and light (L) clayey lime mudstone with low-angle cross beddings. b: faintly laminated mud with lenticular bedding. c: dark mud clast (C) with abrupt lateral contact. small vegetative debris are especially observed in the dark clasts (arrows). d: example of disrupted wavy and lenticular bedding (L). Possible origin of this fabric includes oscillation wave packing or unidirectional current (clast) clustering.

gleysol" (BOULAINÉ, 1992; DUCHAUFOUR, 1977). These aggregates were probably eroded and carried by shifting channels during period of increased Rhône River flooding. They were found in the lower part of the core, then disappeared in the UMM deposit.

—markers of the anthropogenic pollution are microballs and scoriae composed of sulfides and Fe-Al oxides (Figure 11c,d). They were found only in the upper third of the core while talc, another product of human activity resulting from sewage sludge or atmospheric fallout (POPPE *et al.*, 1989 ; RUCH *et al.*, 1989) appeared near 300 cm depth and increased in the top 20 cm of the core (Figure 10).

Interpretation. The period of the channelization of the Grand Rhône can be reliably related to the decrease, then disappearance of ochre aggregates. Channelization was finally completed by 1869 (VIVIAN, 1989). The "wild" Rhône period ended at about 100 cm depth in the core. This depth fairly coincides with the dating deduced from the 0.5 cm y^{-1} average accumulation rate based on ^{210}Pb profiles. The 350 cm transition from LMM to LM corresponds to about 700 yr. B.P., namely

the beginning of the Bras de Fer paleochannel activity, assuming a nearly constant rate through the core. On the mainland, this period was also dated by archaeological tools which indicated marked erosive processes (BRAVARD and BÉTHEMONT, 1989). Consequently, the LMM deposition roughly coincided with the Rhône d'Ulmet branch which was the most important Rhône distributary in the study area. As a consequence, the biological conditions were favorable for the development of benthic organisms and the rates of accumulation were lower. The LM correspond to the successive wild Rhône of Bras de Fer and Grand Rhône branches. The end of their deposition coincides with the disappearance of ochre aggregate markers of the episodic channel displacement. The UMM accumulated essentially during the past century, as indicated by the presence of markers of anthropogenic impact. The modest upcore increase in sands and coarse organic debris (and to some degree of carbonates) may emphasize mark decreasing of flood transport, and therefore an increasing role played by winnowing processes on the marine bottom.

Our data which include radiochemical ages, continental pa-

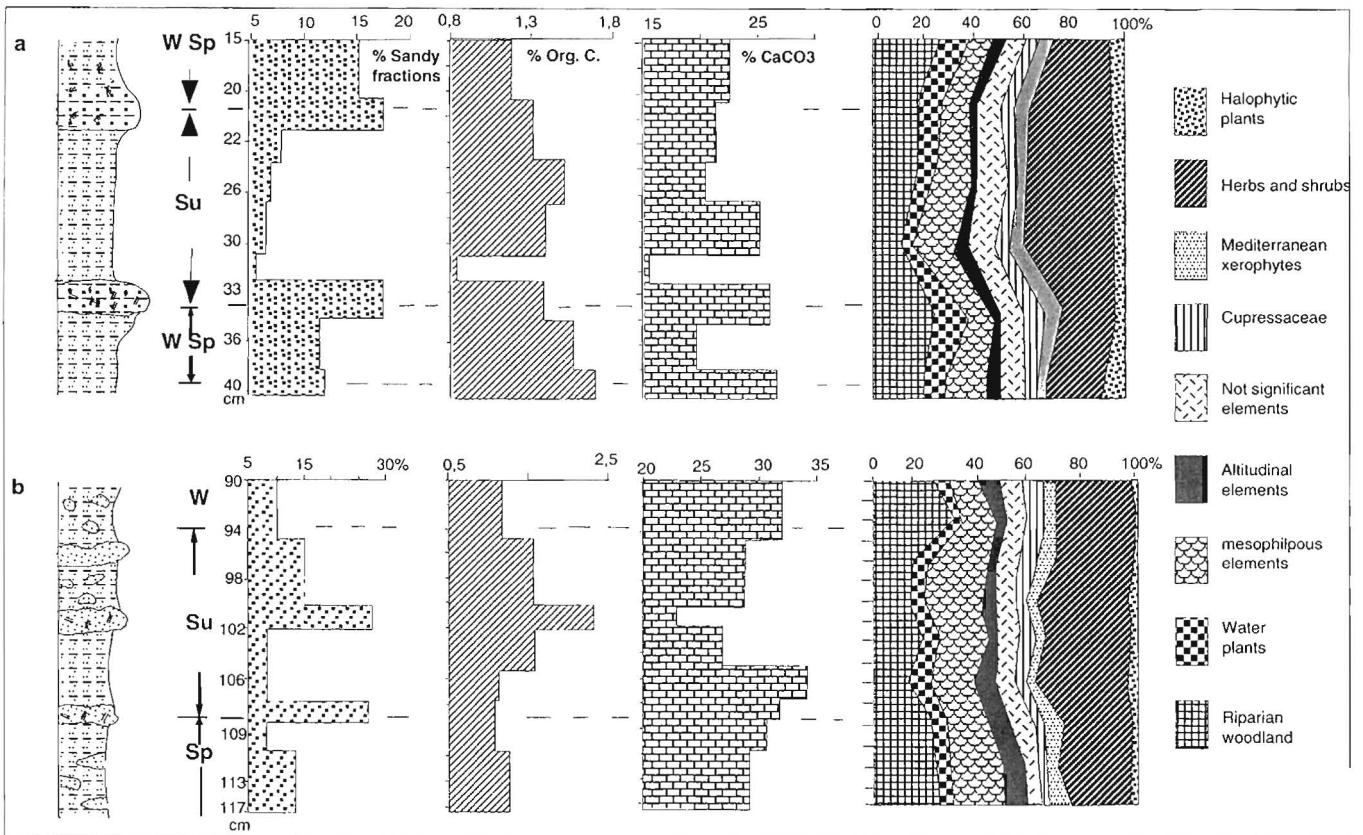


Figure 9. Core-log sketches of laminite sequence, (a) well preserved 40–17 cm interval, (b) faintly preserved 117–90 cm. The pollen assemblages are based on data from SUC *et al.*, 1998, in preparation. W: winter period, Sp: spring period, Su: summer period.

laeoclimatic indices and markers of submarine deposition have a distribution consistent with a coherent stratigraphy.

Regional Lithofacies Correlation and Geometry

The accumulation rates estimated to both ^{210}Pb datings and the 1869 disappearance of ochre aggregates at depth are plotted on the same diagram versus distance from the mouth of Rhône River (Figure 12). This diagram highlights nearly similar curves for the five cores 7 km off the mouth. For the proximal core KTR05 where ochre aggregates were not observed, apparent rates of accumulation were estimated quite similar from both ^{210}Pb and ^{137}Cs profiles.

Period before 1300 A.D. (Rhône d'Ulmet Branch)

Mottled muds were commonly found in the lower part of cores KL03 and KL01. Laminated muds were not observed because of the great distance from the western mouth of Rhône d'Ulmet. Though our cores were not deep enough, we assumed that these laminated muds would have been deposited in the proximal area of the Rhône d'Ulmet prodelta (Figure 6c). The Rhône d'Ulmet was the dominant distributary associated with the diminution of the Saint-Ferreol branch, from the Roman time to High Middle Age (about 500 yrs time interval). During this period, the Rhône hydrosystem seemed

to have changed very slowly in response to low-magnitude climatic variations (BRAVARD, 1983). The runoff pattern and the resulting water supply may be classified as an intermediate value between the present Rhône and the Bras de Fer (PROVANSAL and MORHANGE, 1994).

Wild Rhône Period after 1587 (Bras de Fer and Grand Rhône Branches)

The area of laminated deposits was largely extended during the wild Rhône period than during the Recent one (Figure 6b). Cores KL03, KL01 and K04 display fining upward laminated structures. However they are thinner than the proximal ones. The light layers are less numerous and less delineated. Farther away, at 18 km from the mouth in 80 to 90 m of water, cores K08 and KL04 showed little evidence of lamination. Distinct organic rich laminae (<1 mm) were sometimes present.

In all cores, the top of laminated muds coincided with the drastic disappearance of ochre aggregates, as we saw in the core KL03 example. This double evidence is related to the 1869 regulation of the main channel of the Grand Rhône, when the channel was rectified, fixed, and finally constricted (VIVIAN, 1989). On the basis of the post 1869 sedimentation rate, we dated the beginning of the laminated mud

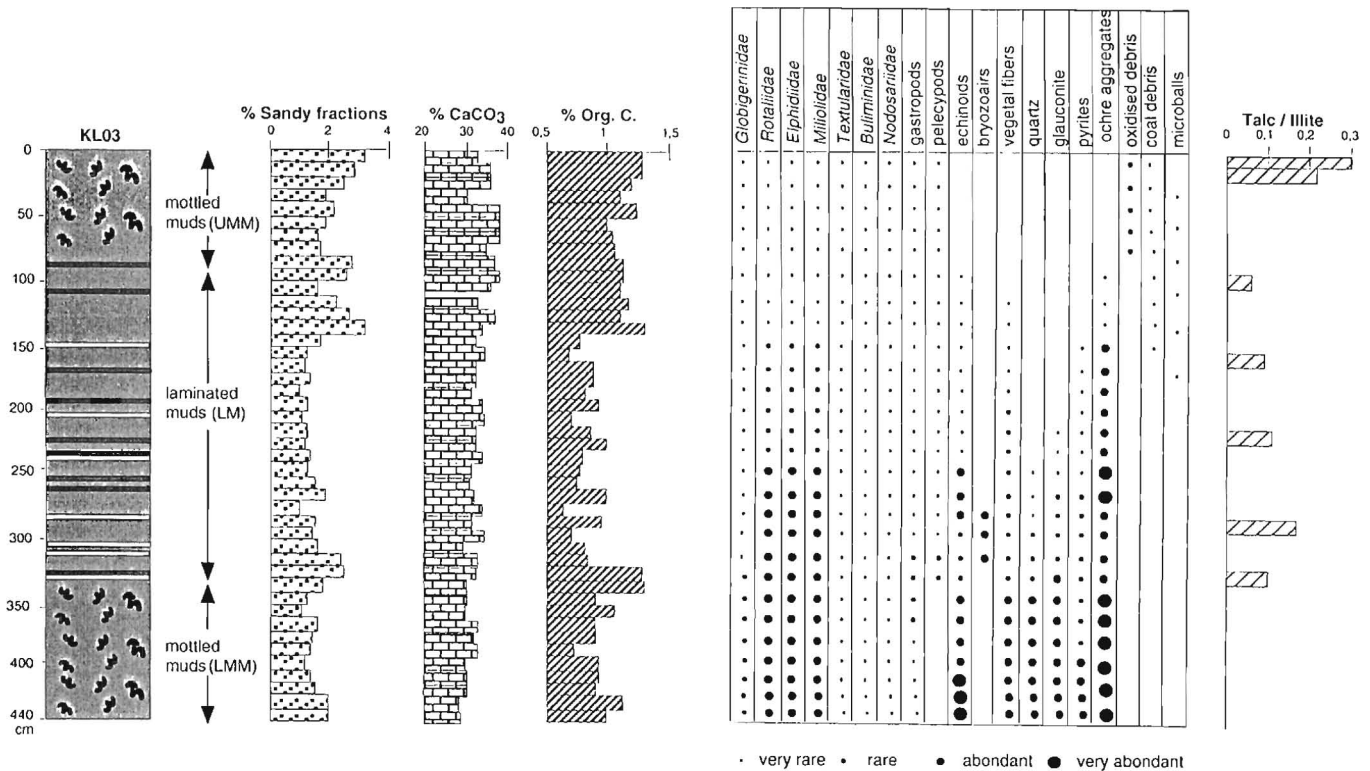


Figure 10. Core KL03—Lithological succession, vertical distribution of sand fraction, carbonates, organic carbon, and of selected environmental markers observed with a binocular microscope. Talc versus illite was evaluated on the basis of the 001 peaks of the $<1 \mu\text{m}$ fraction.

to approximately the 15th century for core KL03 and 13th century for core KL01. The changing climatic conditions modified the watershed, and consequently the channel patterns of the Rhône River during the 15th century (torrential crisis, BRAVARD and BRETEMONT, 1989). This change probably played a prominent role in the initiating the Rhône prodelta sedimentation. On the outer shelf, a $<1 \text{ m}$ thick layer was found to be related to this period which implies a long gap after the 5–6000 yrs deposition.

Recent Period (Channelled Rhône)

The period roughly coincides with the last century and encompasses surficial deposits of the Rhône River after 1869. The proximal KTR05 core shows a succession of dark and light layers, which represent winter floods and summer settling periods. In the most favorable cases, the lamina couplets were preserved and correspond to an annual sequence. This sedimentation microstructure was also observed in other prodeltaic zones of the Mediterranean basin, such as the Nile (SUMMERHAYES *et al.*, 1978, ZHONGHYUAN *et al.*, 1992) and the Ebro Rivers (MALDONADO, 1972). The first ^{137}Cs signal at about 6.94 m indicates that this 7.3 m core section represents approximately the last fifty years. This core was taken 4 km from the mouth. It is the only one which presents laminated structures over the total vertical section and especially in its upper part. Gray mottled muds with dark spots can be identified in the upper part within the neighboring cores (KL03,

KL01) and as far as the distal KL04. These upper muds are characterized by a relatively high sand content that can be attributed to the proximity of the Rhône River source. The high hydrodynamic zone with wave and bottom current interactions resulted in reworking and destruction of the laminae. It is suggested that a longer time of surficial exposure at the sea floor enhanced successive selective removal. On the basis of these data, a larger part of the solid load was assumed to be mostly released in a restricted area which was mapped with the help of two other cores from a previous study (EL HMAIDI, 1993) (Fig. 6a). This deposition in a very proximal area should be considered a result of the impact of all upstream hydroelectric and irrigation structures in the Rhône drainage basin (VIVIAN, 1989).

A simplified stratigraphic fence diagram based on the six cores highlights the facies distribution in time and space (Figure 13).

DISCUSSION

Environmental Significance of Prodeltaic Laminites

The distribution, accumulation and preservation in time and space of laminites were investigated in this study of the Rhône prodelta. Previous detailed studies of this sedimentary structure are few among the world microtidal or mesotidal prodeltas.

Other major microtidal deltas of the Mediterranean margin

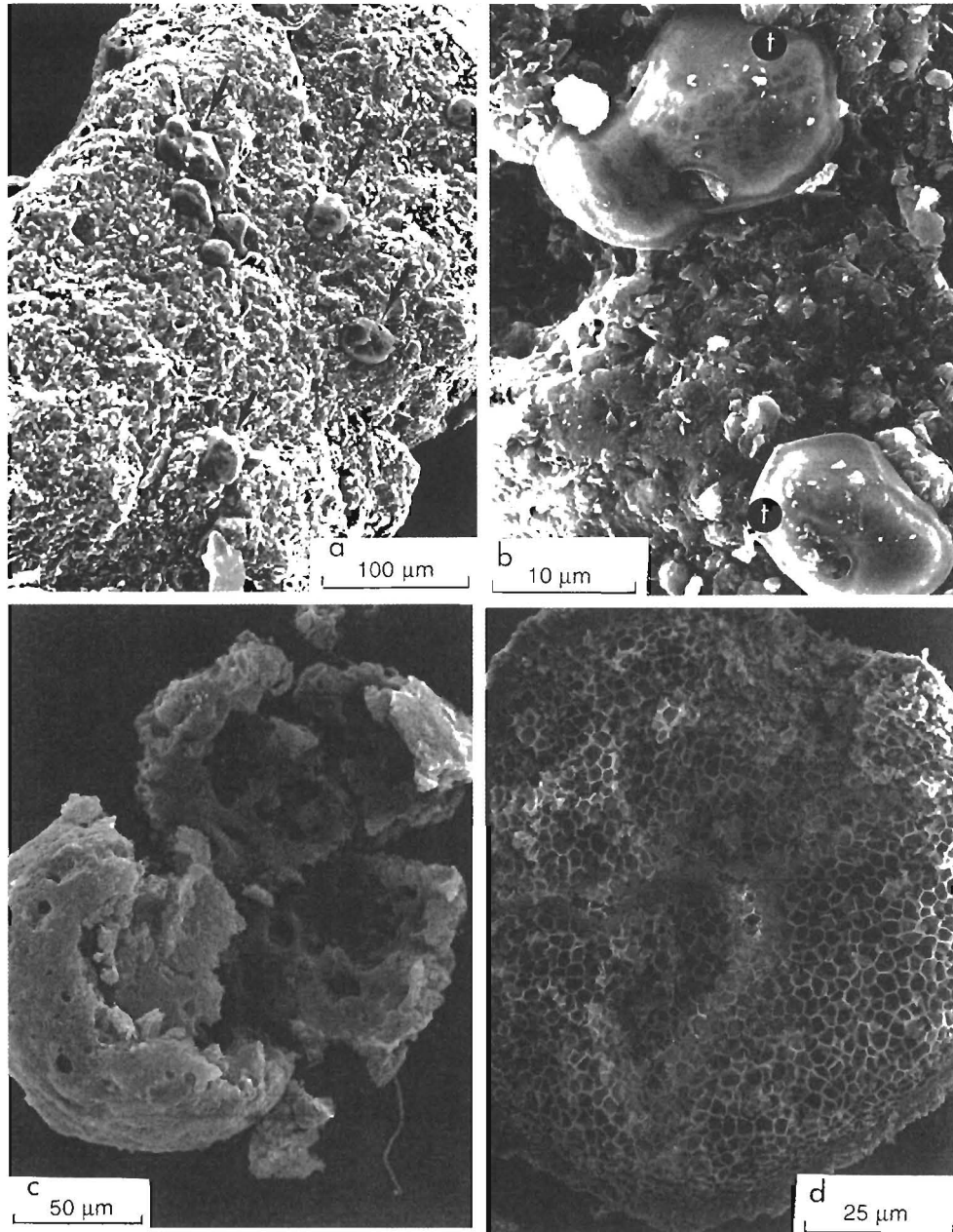


Figure 11. SEM micrographs of environmental markers. a, b: ochre clayey-micritic aggregates of “thionic gleysol” of Rhône delta, local deposition of elemental sulfur—thion (t) (arrows), c, d: different microfabrics of industrial microballs, c: cavernous microballs composed of iron sulfide, K5 05, 30–40 cm, d: honeycomb structure with heterogenous composition (Fe-Al oxides and silica).

(Ebro, Tiber, Nile Rivers) show laminite deposition that can be compared to that of the Rhône River (MALDONADO, 1972; BELLOTI *et al.*, 1994, ZHONGHYUAN *et al.*, 1992). Little is also known about the nature and distribution of these deposits in their subaqueous sites. Clayey silts and silty clays were recognized in the proximal sector of Ebro delta on the basis of obvious organic matter and textural changes: upper laminae were slightly oxidized and lower laminae corresponded to an organic matter-rich unit with dark pigmentation. The outer

sector was characterized by the deposition of vegetal fibers that indicates a distal influence of flood supply. In the Nile delta, 0.5–2 cm thick laminites were described in lagoonal setting or in flood plain of the delta only: alternation of fine sands, silts and sandy muds represents rhythmic flood deposition before the completion of the Aswan High Dam (STANLEY, 1988; ZHONGHYUAN *et al.*, 1992).

Alternations of sandy and muddy laminates off the Mississippi River deltaic plain are usually considered to be the

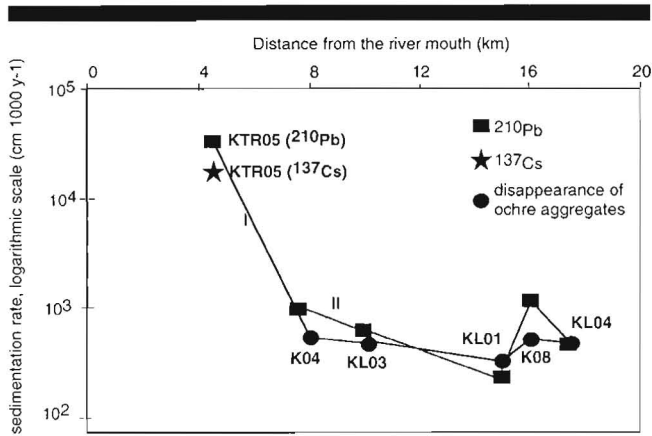


Figure 12. Seaward variation in sediment accumulation rates according to ²¹⁰Pb profiles and a 1869 age of disappearance of ochre aggregates.

products of Mississippi River supply fluctuations (COLEMAN and GAGLIANO, 1965). Seaward, the number and thickness of fine-grained laminae decrease as in the Rhône prodelta and then homogeneous and mottled muds dominate.

The turbid plume on the Amazon shelf is swept north-westward by the North Brazil Current. The residence time for sediment load is dependent also on the easterly trade winds and on the tidal currents (NITTROUER *et al.*, 1995). The occurrence of laminated muds corresponds closely to the areas of rapid sediment accumulation (4–10 cm y⁻¹) in the topset beds region. Dark organic-rich laminae are found on a narrow belt surrounding laminated muds in the topset and foreset bed regions. Seaward, the foreset and bottomset regions where accumulation rates are low (<4 cm y⁻¹) display mottled muds (KUEHL *et al.*, 1995). This process of sedimentation, partly similar to the Rhône process, is characterized, during low tide periods, by a stratified water column. A mud layer forms at the sea bed in association with fluid muds in the water column. The fluid muds result in the settling of material and in the preservation of light layers on the sea bed. During high

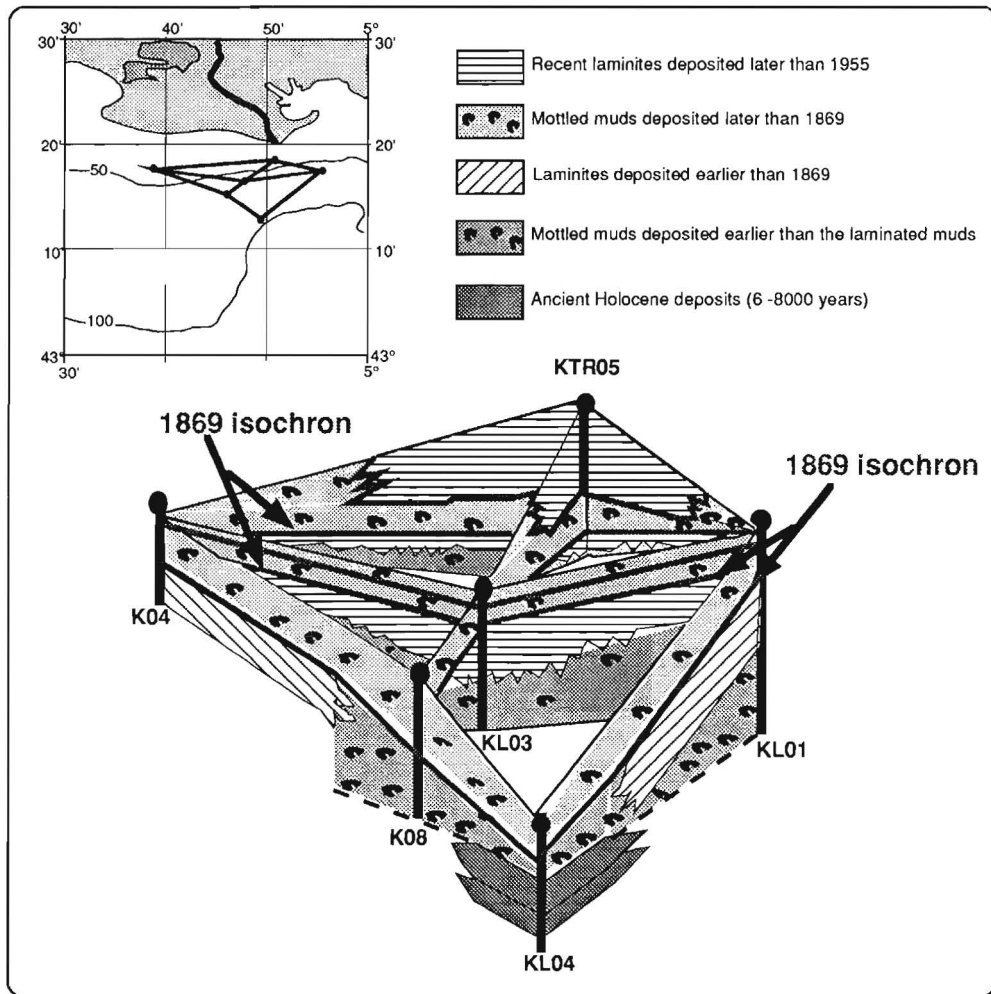


Figure 13. Stratigraphic fence diagram showing facies in time and space across the Rhône prodelta.

tide periods, the water column on the Amazon shelf is mixed. Resuspension and melting of part or all of the fluid mud produce coarser deposits. The presence of a fluid mud layer reduces turbulence and vertical mixing and results in deposition and preservation of the laminated mud (JAEGER and NITROUER, 1994).

In the microtidal area of the Rhône prodelta, the fluid mud (nepheloid layer) is mostly controlled by the fluvial discharge during the flood period. It decreases in thickness, extent and density from the end of the spring season. This would be an important factor in preservation of the complete laminites. Turbulent energy would not be dampened with this thin fluid mud layer on the sea bed. Consequently, the type (*i.e.*, thickness, seasonal record of preservation, truncation) of laminites would depend upon not only sediment supply, but also energetic factors.

Recent Evolution of the Rhône Prodeltà System: Anthropogenic Effects

The Rhône represents a good example of a large European river that has been influenced by human influence over several hundred years. Archaeological evidence indicate a dramatic increase in progradation after 15th century AD that would have resulted more from the climatic impact of the Little Ice Age than from anthropogenic action. Sediment supply was modified at the same time by deforestation and agriculture. The same sequence can be observed in the drainage area of the Tiber River with frequent and intense floods between the 15th and 19th centuries (BELLOTI *et al.*, 1994).

The human activities have increased remarkably since the middle of the 1800s. In the Rhône River, major impacts are due to civil engineering works implemented to facilitate navigation, to protect towns and lands against floods and, above all, to produce energy. This anthropogenic influence has drastically modified the flow regime and sediment load, then inducing shoreline retreat, and prodeltaic depocenter migration (2nd order impact). The same evolutionary trend can be observed from the Danube River (BRAVARD and BÉTHEMONT, 1989; PECSI, 1968) and the Rhine River (CARBIENER, 1983; FIEDRICH and MULLER, 1984). In the Nile delta also, during the past two centuries, acceleration of irrigation and land reclamation projects, and intensification of agriculture have diminished the surface area of the lagoonal and marsh environments (ARBOUILLE and STANLEY, 1991).

The discharge values and the chronological series of the Rhône River indicate that significant change occurred since 1950 owing to (1) the building of hydroelectric dams and (2) reforestation and river-bed quarrying, taking away most of the sediment that normally nourishes the deltaic shoreline and the prodeltaic deposition. In the Tiber delta also, the beaches have been deprived of fluvial sediments for the past 40 years because of the construction of five hydroelectric dams (BELLOTI *et al.*, 1994). One of the best evidence of anthropological influence is the closure of High Aswan Dam on the Nile River in 1964 which result in changes in deltaic environment, reduced fine sediment supply from the coast to the inner shelf: the coupling of erosion by bottom currents and reduced sediment input from the Nile is likely to have

induced depositional changes on the shelf (STANLEY, 1988). The similar consequence was illustrated by this study on the Rhône prodelta: the upward coarsening observed in the upper part of cores KTR05, K04, KL03 and KL01 largely result from this degenerative trend

CONCLUSIONS

The present Rhône prodelta deposition is characterized by the seasonal build-up of laminites which is mostly controlled by the fluvial discharge during the flood period. This accumulation is altered seaward with the decrease in volume and density of the nepheloid layer from the end of the spring season: faintly laminated muds and mottled muds were successively deposited on the mid and outer shelf. Because a longer time of exposure, the deposits of this distal prodelta provided evidence of seasonally-intensified wave erosion.

Before 1300 y.A.D. and due to a north-western location of the main river mouth and low magnitude of floods, mottled mud predominated in the present prodelta area. During the XVI–XIXth centuries interval ("wild" Rhône period), an eastward prodeltaic depocenter migration and a dramatic extent of the laminated muds would have resulted more from the climatic control than from anthropogenic impact. However, sediment fluxes were enhanced at the same period by deforestation and agriculture. The anthropogenic influence has increased since the middle of the 1800s then inducing discharge modification but the most significant change occurred since 1950: building of dams and river-bed quarrying, individually or in combination, are the primary generators of the reduced sediment input.

ACKNOWLEDGEMENTS

This work was supported by the Programme National d'Océanographie Côtière—ÉCOsystèmes CÔTiers (PNOC—ECOCOT). We are grateful to Mrs Brigitte Deniaux who helped us with the English language of the manuscript.

LITERATURE CITED

- ALESSANDRO, V.; BARTOLINI, C.; CAPUTO, C., and PRANZINI E., 1990. Land use impact on Arno Ombrone and Tiber deltas during historical times. *In*: QUELENNEC, R.E., ERCOLANI, E., and MICHON, G. (eds), *Littoral 1990*, Eurocoast, Chateau-Gombert, Marseille, pp. 261–265.
- ALOISI, J.C.; MILLOT C.; MONACO, A., and PAUC, H., 1979. Dynamique des suspensions et mécanismes sédimentométriques sur le plateau continental du Golfe du Lion. *C.R. Acad. Sci. Paris*, 289, 879–882.
- ARBOUILLE, D. and STANLEY, D.J., 1991. Late Quaternary evolution of the Burullus lagoon region, north-central Nile delta, Egypt. *Marine Geology*, 99, 45–66.
- BALTZER, F., 1980. Géodynamique de la sédimentation et diagenèse précoce sur un delta tropical à mangroves en domaine ultrabassique (Nouvelle-Calédonie). Thèse Sci., Univ. Paris-Sud, Orsay.
- BELLOTI, P.; CHIOCCI, F.L.; MILLI, S.; TORTORA, P., and VALERI, P., 1994. Sequence stratigraphy and depositional setting on the Tiber delta: integration of high-resolution seismics, well logs, and archaeological data. *Journal. Sedimentary Research*, B64, 3, 416–432.
- BLANC, J.J. and JEUDY DE GRISSAC, A., 1982. Dangers de l'érosion littorale en Petite Camargue (Aire occidentale du delta du Rhône, France). *Thetys*, 10(4), 349–354.
- BLANC, J.J., 1977. Recherche de sédimentologie appliquée au littoral du delta du Rhône de Fos au Grau du Roi. *Contrat CNEXO*, Paris, 75/1193, 69p.

- BOULAIN, J., 1992. *Typologie des sols*. Coll. Sols, INA, Paris-Grignon, 8, 139 pp.
- BRAVARD, J.R., 1983. Les sédiments fins des plaines d'inondation dans la vallée du Haut-Rhône (approche qualitative et spatiale). *Rev. Géogr. Alpine*, 71, 363–379.
- BRAVARD, J.R. and BÉTHEMONT, J., 1989. Cartography of rivers in France. In: PETIT, G.E. et al. (eds), *Historical change of large alluvial rivers: Western Europe*, Chichester: Wiley, pp. 95–111.
- BRENCHLEY, P.J. and NEWALL, G., 1977. The significance of conformed bedding in the Upper Ordovician sediments of the Oslo region, Norway. *Journal Sedimentary Petrology*, 47, 819–833.
- CARBIENER, R., 1983. Le grand Ried central d'Alsace: écologie et évolution d'une zone humide d'origine fluviale rhénane. *Bull. Ecol.*, 14(4), 249–277.
- COLEMAN, J.M. and GAGLIANO, S.M., 1965. Sedimentary structures: Mississippi River deltaic plain. In: MIDDLETON, G.V. (ed.), *Primary Sedimentary Structures and Their Hydrodynamic Interpretation*, SPEM, sp. publ., Tulsa, 12, 133–148.
- COUPELLIER, V. and STANLEY, D.J., 1987. Late Quaternary stratigraphy and paleogeography of the eastern Nile delta, Egypt. *Marine Geology*, 77, 257–275.
- DEMARCO, H. and WALD, L., 1984. La dynamique superficielle du panache du Rhône d'après l'imagerie infrarouge satellitaire. *Oceanologica Acta*, 7, 159–162.
- DUBOUL-RAZAVET, C., and KRUIT, C., 1957. Sédimentologie du delta du Rhône. *Rev. Inst. Français Pétrole et Ann. Combustibles liquides*, XII, 4, 399–410.
- DUCHAUFOUR, P., 1977. *Pédologie. 1: Pédogenèse et classification*, Masson éd., 453 pp.
- DURRIEU DE MADRON, X., and PANOUZE, M., 1996. Transport de matière particulaire en suspension sur le plateau continental du Golfe du Lion. Situation estivale et hivernale. *C.R. Acad. Sci. Paris*, 322, IIa, 1061–1070.
- DURRIEU DE MADRON, X.; ABASSI, A.; HEUSSNER, S.; MONACO, A.; ALOISI, J.C.; RADAKOVITCH, O.; GIRESE, P.; BUSCAIL, R., and KERHERVE, P., 2000. Particulate matter and organic carbon budgets for the Gulf of Lions (NW Mediterranean). *Oceanologica Acta*, 23, 6, 717–730.
- EL HMAIDI, A., 1993. Unités sédimentaires et paléoenvironnements sur la marge rhodanienne (Golfe du Lion, France). Thèse Doct., Univ. Perpignan, 174 pp.
- ESTOURNEL, C.L.; KONDRACHOFF, V.; MARSALÉIX, P., and VEHIL, R., 1997. The plume of the Rhône: numerical simulation and remote sensing. *Continental Shelf Research*, 17, 8, 899–924.
- FRIEDRICH, G. and MULLER, D., 1984. Rhine. In: WHITTON, B.A. (ed.), *Ecology of European Rivers*, Blackwell, London, pp. 265–315.
- GENSOU, B. and TESSON, M., 1996. Sequence stratigraphy, seismic profiles, and cores of Pleistocene deposits on the Rhône continental shelf. *Sedimentary Geology*, 105, 183–190.
- JAEGER, J.M. and NITTROUER, C.A., 1994. Tidal controls on the formation of fine-scale sedimentary strata near the Amazon river mouth. *Marine Geology*, 125, 259–281.
- KUEHL, S.A.; NITTROUER, C.A., and RINE, J.M., 1995. Seabed dynamics of the inner Amazon continental shelf: temporal and spatial variability of surficial strata. In: NITTROUER, C.A. and KUEHL (ed.), *Geological significance of sediment transport and accumulation on the Amazon continental shelf*. *Marine Geology*, 125, 283–302.
- LAMB, H.H., 1996. *The changing climate*, Methuen, London, 236 pp.
- L'HOMER, A.; BAZILE, F.; THOMMERET, J., and THOMMERET, Y., 1981. Principales étapes de l'édification du delta du Rhône de 7000 BP à nos jours; variations du niveau marin. *Oceanis*, 7, 4, 389–408.
- L'HOMER, A., 1992. Sea-level changes and impacts on the Rhône delta coastal lowlands. In: TOOLEY, M.J. and JELGERSMA, S. (eds), *Impact on sea-level rise on European coastal lowlands*, Blackwell, UK, pp. 136–152.
- MALDONADO, A., 1972. El delta del Ebro. Estudios sedimentológico y estratigráfico. Boletín de Estratigrafía, 1, Ph. D. Thesis, University of Barcelona, 450 pp.
- MILLMAN, J.D.; QUIN, Y.S.; REN, M.E., and SAITO, Y., 1987. Man's influence on the erosion and transport of sediment by Asian rivers: the Yellow River (Huanghe) example. *Journal of Geology*, 95, 751–762.
- MILLOT, C., 1990. The Gulf of Lions hydrodynamics. *Continental Shelf Research*, 10, 885–894.
- NITTROUER, C.A.; KUEHL, S.A.; STERNBERG, R.W.; FIGUEIREDO, A.G., and FARIA, L.E.C., 1995. An introduction to the geological significance of sediment transport and accumulation on the Amazon continental shelf. *Marine Geology*, 125, 177–192.
- PECSI, M., 1968. Evolution of the flood plain levels of the Danube and their principal bearing on the geography of agriculture. *Ac. Sc. Hungarica*, Inst. Geogr., Fold. Kozl., 3, 215–222.
- PONT, D., 1992. Caractérisation de la charge solide en suspension du Rhône au niveau du palier d'Arles lors d'une crue d'importance moyenne. *Rapport final, Agence de l'eau Rhône-Méditerranée-Corse*, Univ. Lyon II, 25 pp.
- PONT, D., 1993. Vers une meilleure connaissance des apports du Rhône à la Méditerranée. *Les rencontres de l'Agence Régionale pour l'environnement, Provence-Alpes-Côte d'Azur*, Marseille, 16–24.
- PONT, D., 1997. Les débits solides du Rhône à proximité de son embouchure: données récentes (1994–1995). *Revue de Géographie de Lyon*, 72, 23–33.
- POPPE, L.J.; HATHAWAY, J.C., and ARMENTER, C.M., 1989. Talc in the suspended matter of the Northwestern Atlantic. *Clays and Clay Minerals*, 31, 1, 60–64.
- PROBST, J.L., 1989. Hydroclimatic fluctuations of some European Rivers since 1800. In: PETIT, G.E. et al. (eds), *Historical change of large alluvial rivers: Western Europe*, John Wiley and Sons, Chichester, pp. 41–55.
- PROVANSAL, M. and MORHANGE, C., 1994. Seuils climatiques et réponses morphogéniques en Basse-Provence depuis 5000 ans. *Quaternaire*, 5 (3–1), 113–118.
- RADAKOVITCH, O., 1995. Étude du transfert du matériel particulaire par le ^{210}Po et ^{210}Pb . Applications aux marges continentales du Golfe de Gascogne (NE Atlantique) et du Golfe du Lion (NW Méditerranée). *Doct. thesis, Univ. Perpignan*, 185 pp.
- RADAKOVITCH, O., CHARMASSON, S., ARNAUD, M., and BOUISSET, J., 1999. ^{210}Pb and caesium accumulation in the Rhône delta sediments. *Estuar. Coast. Shelf Sci.* 48, 77–92.
- RIVIERE, A., 1977. *Méthodes granulométriques. Techniques et interprétations*. Masson, Paris, 164 p.
- RODITIS, J.C. and PONT, D., 1993. Dynamiques fluviales et milieux de sédimentation du Rhône à l'amont immédiat de son delta. *Méditerranée*, 3–4, 5–18.
- RUCH, P.; BAPST, A., and KUBLER, B., 1989. Talc: an indicator of recent anthropogenic activity. *Clay Minerals*, 24, 33–42.
- SAVEY, P. and DELEGLISE, R., 1967. Les incidences de l'aménagement du tiers central du Rhône sur les transports solides en suspension. *Ass. Int. Hydrol. Scient. Publ.*, 75, 462–476.
- SCHMITTNER, K.E. and GIRESE, P., 1999. Micro-environmental controls on biomineralization: superficial processes of apatite and calcite precipitations. Quaternary soils, Roussillon, France, *Sedimentology*, 46, 463–476.
- SOGREAH, (Société Grenobloise de Recherches et d'Etudes des Actions Hydrauliques) 1994. Rapport d'activités sur l'étude de l'évolution du littoral sableux de la Camargue, Grenoble, 1–5, 96 pp.
- SUC, J.P.; CAMBON, G.; TOUZANI, A.; GIRESE, P.; ALOISI, J.C.; SUBALYOVA, D.; MARSET, T.; SERVE, L.; GADEL, F.; FAUQUETTE, S.; ARNAUD, M.; CHARMASSON, S.; COCHONAT, P.; DUZER, D.; FERRI, J., and ROBERT, J.P., 2000. Present-day rhythmic deposition in the Grand Rhone prodelta (NW Mediterranean); High resolution analysis of the core KTR05, in preparation.
- STANLEY, D.J., 1988. Low sediment accumulation rates and erosion on the middle and outer Nile delta shelf of Egypt. *Marine Geology*, 27, 43–65.
- SUMMERHAYES, C.P.; SESTINI, G.; MISDORP, R., and MARKS, N., 1978. Nile delta: Nature and evolution off continental shelf sediments. *Marine Geology*, 27, 43–65.
- THUNUS, V., 1996. Modélisation à méso-échelle de l'hydrodynamisme et du transport de particules en milieu marin semi-ouvert. Application au Golfe de Lion. Thèse de Doctorat, Univ. de Neuchâtel, 152 pp.
- VARELA, J.M.; GALLARDO, A., and LOPEZ DE VELASCO, A., 1986. Retención de sólidos por las presas de Mequinenza y Ribarroja. Efec-

- tos de los aportes en el Delta del Ebro. In: MARINO, M.G. (ed), *El sistema integrado del Ebro*; Hermes, Madrid, pp. 203–219
- VIVIAN, H., 1989. Hydrological changes of the Rhône River. In: PETIT, G.E. (ed), *Historical change of large alluvial rivers: Western Europe*, John Wiley and Sons, Chichester, PP. 57–93.
- WALTER, A.V; SIMONNET, J.P., and PONT, D., 1997. Evolution and modelization of the suspended sediment discharge of the Rhône River (France). Consequences of catchment heterogeneity, river management and climatic variability. *6th Congr. Français de Sédimentologie*, Publ. A.S.F., Paris, 27, 279–280.
- WELCOMME, R.L., 1978. *Fisheries Ecology of the Flood plain Rivers*, Longman, London, 297 pp.
- ZHONGHYUAN, C.; WARNE, A.G., and STANLEY, D.J., 1992. Late Quaternary evolution of the Northwestern Nile delta between Rosetta Promontory and Alexandria, Egypt. *Journal of Coastal Research*, 8, 3, 527–561.